PATCHING HELE-SHAW CELLS TO SIMULATE SILICA SCALE DEPOSITION IN DISCRETE FRACTURE NETWORKS

Pouria Aghajannezhad[1], Mathieu Sellier[1]

[1]Department of Mechanical Engineering, University of Canterbury, Christchurch, New Zealand

Keywords: *Silica Deposition, Computational Fluid Dynamics, Hele-Shaw Cell, Discrete Fracture Network*

ABSTRACT

Due to mineral deposition in geothermal reservoirs, the electrical production of geothermal power plants decreases over time. Specifically, silica can form extremely hard and dense scales not only in power-plant equipment and pipelines but also within and around wells, restricting flow and reducing power-plant efficiency. Understanding the effect of silica scaling on flow rates can inform the required maintenance during different stages of the geothermal plant lifetime. Accordingly, a detailed analysis of silica scale growth offers powerful insight to predict the productive lifetime of the reservoir and mechanical infrastructures. Fluid within many geothermal reservoirs is largely transported along a network of fractures. However, available simulation methods to study mineral deposition within large-scale fracture networks are computationally expensive. We have developed a new modeling framework based on representing individual fractures using the Hele-Shaw cell analogy and simulating fracture networks by connecting these Hele-Shaw cells together using pressure constraints at intersecting nodes of the computational mesh. This methodology allows the rapid computation of flows in realistically large fracture networks. This paper will discuss how this modeling framework can be used to study the transport of diluted specious in rock fractures, which provides a backbone for the simulation of silica scale deposition in a discrete fracture network.

1. INTRODUCTION

Extreme temperature changes are a common cause of rock fracture formations (Feng et al. 2017). Most formed fractures are intersected with one another, providing functional spaces to carry subsurface water. A significant number of geoengineering problems can be addressed by modeling fluid flow and solute transport in these rock fractures, such as the prediction of geothermal reservoir lifetime. For studying the behavior of fluid flow in rock fractures specifically at the intersections, a wide range of methods have been developed (Yu, Liu, and Jiang 2017). Models based on the Navier-Stokes Equations (NSE) and the Cubic Law (CL) have attracted considerable interest, the NSE due to their accuracy and the CL due to its simplicity. However, it is computationally demanding to solve the NSE coupled with the advective-diffusion equation. Also, the CL cannot provide satisfactory results. The CL is an additional simplification of the Hele-Shaw equation that applies when the flow is invariant in the flow direction and states that the flow rate through parallel plates has a cubic relation with the plates' aperture. Accordingly, to achieve relatively accurate predictions of hydraulic resistance and solute concentration through a fracture network, very simplified methods are inadequate and very complex methods are computationally expensive. Consequently, a less demanding and better-conditioned modeling framework should be adopted.

Due to the computational costs of including topological features on rock fractures, many researchers have relied on simplified models, which consider smooth parallel surfaces (Wu et al., 2018). Therefore, a precise solution for this problem can be provided by considering the effect of surface roughness on the fluid flow and solute transport in multiple intersected fractures. Since natural rock fractures are composed of rough walls, the formation of complex topological patterns at the intersections is inevitable. In some cases, surface roughness at an intersection leads to a decrease in aperture size. There might be other possible consequences, such as flow stirring. Adequate proof of higher stirring rate in the laminar flow regime as a consequence of surface corrugation is presented in recently developed research (Gepner and Floryan 2020). Roughness characteristics and dimensions can be obtained by scanning real rock fractures. However, because of the inaccessibility of natural rock fractures, it is impractical to scan a large-scale fractured system with digitized surface scanners.

Various approaches have been applied to generate random topologies (Huang, Cao, and A 2017). Some preliminary work was carried out on the generation of random Gaussian surfaces in the late 1970s (Patir 1978). In that work, an algorithm to represent real surfaces was presented. This algorithm is based on two predefined parameters for the surface roughness: the autocorrelation and frequency density functions of the surface. De Castro et al. (2017) examined Gaussian surface roughness using Fourier analysis. Fabbro et al. (2006) proposed a new method for defining the surface roughness based on the certain frequency of the surface oscillation. In their approach, characteristics of surface roughness were determined with respect to its spatial frequency quantity. This method is based on solving the wave equation by using the mixed Fourier transform.

Hele-Shaw (HS) cells are defined as confined spaces between two parallel plates in close proximity (Saffman 1986), which represents the rock fracture. HS cells are recognized as one of the most efficient approaches for simulating fluid flow between parallel plates (de Santiago et al. 2020). Studies of solute transport considering the effect of surface roughness using HS cells are scares and the majority of studies used HS equation for modeling viscous fingering patterns (Morrow, Moroney, and McCue 2019), heat transfer (Letelier, Mujica, and Ortega 2019) and multiphase flow in rock fractures (Hu et al. 2019). Transport with low-density contrast was modeled by Oltean et al. (2004). Despite the lack of surface roughness effect, the dilute solution behavior into HS cell was modeled in a good agreement with the experiment. The HS cells became validated by Oltean et al. (2008) to model variable-density flow. However, there is still a need for better quantification of scaling, which becomes available by coupling hydrodynamics into salute transport.

Initial simulation of silica scaling was carried out in the mid-80s (Lai, Bovarsson, and Witherspoon 1985). This work has found that the deposition is dependent on the chemical and thermal process. The recent development regarding

ISSN 2703-4275

modeling the silica deposition in rock fractures has led to a better understanding of surface roughness effects on the deposition. For instance, Van den Heuvel et al. (2020) studied the effect of surface roughness on the silica deposition using different materials. They concluded that rougher surfaces have higher rates of silica deposition. Hai Huang et al. (2020) reported a new visual method for studying the transport in rough fractures. They found that surface roughness causes a high degree of uncertainty associated with transport in rough vertical fractures. Several authors have used the advection-diffusion equation coupled with NSE to model transport in the rock fracture (Deng et al. 2015; Li et al. 2019; Wang and Cardenas 2015). Although these approaches are interesting, they fail to obtain results computationally efficiently.

This paper outlines a computationally efficient approach for modeling fluid flow and solute transport in natural rock fractures that is the basis for modeling the silica deposition. Notably, our findings will be beneficial for having a better understanding of the surface roughness effect on solute transport and fluid flow behavior. This paper presents a new model to describe the behavior of diluted fluid flow through single rough-walled and smooth-walled fractures. The numerical models were implemented within the COMSOL Multiphysics software package. We investigate the accuracy of a simplified modeling approach, which is based on the Hele-Shaw approximation, by comparing it with the NSE. As mentioned before, this paper aims to provide a better quantification of scaling by coupling hydrodynamic into solute transport.

2. METHODOLOGY

2.1 Governing equations

2.1.1 The Navier-Stokes Equations

The Navier-Stokes equations (NSE) and mass conservation for single-phase, laminar, incompressible flow can be described by the following equations:

$$\frac{\partial \boldsymbol{u}}{\partial t} + (\boldsymbol{u} \cdot \nabla)\boldsymbol{u} = -\frac{1}{\rho}\nabla P + \frac{\mu}{\rho}\nabla^2 \boldsymbol{u} \qquad \text{Eq. 1}$$

$$\nabla . \boldsymbol{u} = 0 \qquad \text{Eq. 2}$$

In these equations, t denotes time, ρ is the fluid density (kg/m^3), $\boldsymbol{u} = [u, v, w]$ is the velocity vector (m/s), P is the pressure (Pa), and μ is the viscosity (Pa·s). In the following, we assume water which is at 20°C, and has $\rho = 10^3$ kg/m^3 and $\mu = 10^{-3}$ Pa·s. The values of utilized parameters in this study are given in Table1.

2.1.2 The advection-diffusion equation

The governing equation of solute transport is the general advection-diffusion equation (Bundschuh and Suárez Arriaga, 2010):

$$\frac{\partial C}{\partial t} = -\boldsymbol{u} \cdot \nabla C + \nabla \cdot (\mathrm{D}\nabla \mathrm{C}) \qquad \text{Eq. 3}$$

Where C (mol/m^3) is the volumetric solute concentration and D (m^2/s) is the molecular diffusion coefficient.

2.1.3 The Hele-Shaw equation

In order to simplify the NSE, we made the following assumptions: Above all, the flow is assumed to be laminar. The inertia forces are considered to be negligible in comparison with viscous forces and pressure forces. Lastly, flow is averaged across the fracture aperture and described by the velocity $\boldsymbol{V} = [v, w]$. Consequently, the computational domain was converted using depth averaging from a three-dimensional domain with a three-component velocity field into a two-dimensional computational domain, thus significantly reducing the computational requirements. As a result, the neater governing equations (Hele-Shaw) for explaining the behavior of the fluid flow between parallel plates separated by (h), which is the fracture aperture, is revealed in Equation 5 (Gordon 1983). As mentioned before, the computational domain reduces three-dimensional into two-dimensional, which reduces the computational requirement.

$$\boldsymbol{V} = -\frac{h^2}{12\mu}\nabla P \qquad \text{Eq. 4}$$

$$\nabla \cdot (h\boldsymbol{V}) = 0 \qquad \text{Eq. 5}$$

The approximated velocity $\boldsymbol{V}$ was used for determining the solute concentration in Equation 3. In other words, $\boldsymbol{u}$ was replaced by $\boldsymbol{V}$. The Reynolds number for the flow within fractures is given by

2.1.4 Reynolds number and hydraulic resistance

$$Re = \frac{\rho Q}{\mu W} \qquad \text{Eq. 6}$$

W is the fracture width perpendicular to the direction of the bulk flow. The hydraulic resistance R (Pa·s^1·m^{-3}) is calculated by

$$R = \frac{\Delta P}{Q} \qquad \text{Eq. 7}$$

2.1.5 Surface roughness generation

The pressure difference between inlet and outlet is given by ΔP (Pa), which is named the global pressure difference, and Q represents the flow rate (m^3/s). The generation of surface roughness was done by employing a trigonometric series(Barnsley et al., 1988). This technique is based on the Fourier series, which can characterize surface roughness with respect to the wavenumber quantity. The generally accepted utilization of this approach refers to its reasonable outcomes for creating rough-walled fractures (Fabbro et al., 2006). The surface roughness can be generated using the following double sum:

$$f(x,y) = \sum_{m=-M}^{M}\sum_{n=-N}^{N} a(m,n)\cos\big(2\pi(mx+ny) + \varphi(m,n)\big) \qquad \text{Eq. 8}$$

In this equation, x and y are the spatial coordinates, m and n are the wavenumbers, $a(m,n)$ are amplitudes, and $\varphi(m,n)$ are phase angles. . It should be noted that f in Eq. 11 is describing the location of the upper and lower surface of each fracture. Different values of amplitude can generate different rates of rough surfaces. Hence, by varying this value, a variety of geometrical surfaces with different tortuosities were produced.

2.1.6 Surface roughness characterization

For measuring the surface roughness, a wide scope of approaches are available (Zhang et al., 2017). Nevertheless, Joint Roughness Coefficients (JRCs) have been broadly used in the past ten years (Li et al., 2016). Therefore, a MATLAB code was developed based on Equations 9 and 10 for the

evaluation of surface roughness. The evaluated JRCs are in the range of 0.59–7.21.

$$JRC = 32.2 + 32.47\log Z_2 \quad \text{Eq. 9}$$

Here Z_2 is a dimensionless quantity for measuring the roughness and is defined by the following the root mean square:

$$Z_2 = \left[\frac{1}{M}\sum\left(\frac{z_{i-1}-z_i}{x_{i-1}-x_i}\right)^2\right]^{1/2} \quad \text{Eq. 10}$$

Here M represents the number of points along the fracture width (, z_i and x_i are the coordinates of the fracture surface. For obtaining Z_2, the (x, z) coordinates of several points were evaluated from mid-cross-section of the generated fractures (i is indicating the number of points). In general, $Z_2 = 0$ indicates a smooth-walled fracture, while $Z_2 = 0.5$ indicates the roughest surface in nature, which approximately represents JRCs changing from 1 to 20. In this study Z_2 was chosen in the range of 0.106 to 0.17. The influence of roughness on the fluid flow is stronger when the JRC is higher.

2.1.7 Peclet number

For keeping the stability of the solution, the calculated Peclet number for each simulation was monitored. The Peclet number, *Pe*, represents the ratio between convective and diffusive rates and is given by

$$Pe = \frac{Q}{WD} \quad \text{Eq. 11}$$

2.2 Numerical methodology

We used the COMSOL Multiphysics software package to run the simulations for this study. Two modules were used for solving the NSE (Eq. 1) and HS (Eq. 5); those modules are the single-phase laminar flow interface and the coefficient form boundary PDE, respectively. Furthermore, different solvers and algorithms were employed for solving these two equations. For the HS, a time-dependent solver and the MUMPS direct linear-system solver were used, and for the NSE, the time-dependent algebraic multigrid solver and the generalized minimal residual GMRES linear-system solver were utilized. For the NSE approach, The domain was discretized using tetrahedral and quad. Quadratic shape functions are used for the velocity field and linear ones for the pressure. Moreover, cubic elements with Lagrange shape functions were performed for discretization in the HS models.

For numerical stability and mesh-independency, a mesh sensitivity study was conducted. For the sake of conciseness, the results of this study are not shown here. It is important to note that the NSE are solved in a 3-dimensional domain, whereas the simplifications made in deriving the HS equation result in a 2-dimensional surface domain — the third dimension representing the direction of the aperture (the thickness of the fracture) is accounted for in the governing equations. For the HS simulations, the velocity and hydraulic resistance had to be derived from the solved pressure gradient using Equation 4.

Table 1: Fluid properties in simulations.

Parameter	Symbol	Value
Fluid density	ρ (kg/m^3)	997
Viscosity	μ (Pa·s)	8.9×10^{-4}
Diffusion coefficient	D (m^2/s)	2.03×10^{-9}
Global pressure difference	ΔP (Pa)	0.01
Peclet number	$Pe\ (-)$	10-100
Reynolds number	$Re\ (-)$	0.08-1

2.3 Geometry and boundary conditions of the computational model

As the study's focus was on the transport of diluted species in the rock fractures, which could represent silica, a new model was presented for this investigation. This model consists of one single fracture for which we consider different degrees of surface roughness. As was stated earlier, the generation of surface roughness was done by changing the amplitudes in Equation 8. The fracture is 1 m wide and 1 m long, and the mean fracture aperture is 0.02 m. It should be noted that the fracture aperture is constant in both models.

The boundary conditions were defined as follows. For the inlet and outlet boundaries, a constant pressure Dirichlet boundary conditions were applied over the inlet and outlet edges of the fracture in the Hele-Shaw (HS) approximation, and over the inlet and outlet surface areas of the fracture in the Navier-Stokes approach. The general advection-diffusion equation was solved by coupling it with the HS equations and NSE. The computational domain is depicted in Figure 1, with colour-coded boundary conditions. The blue arrows indicate the inlet flow and the orange arrows indicate the outlet flow. The pressure difference between the inlet and outlet is called the global pressure difference. The red line in Figure 1 is specified for extracting data which is situated at a distance of 0.3 m from the inlet. A mineral concentration of100 mol/m^3 was applied at the inlet boundary.

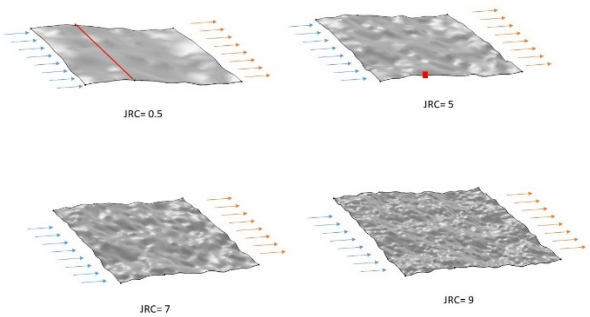

Figure 1: The geometrical patterns of single fractures generated for studying the effect of surface roughness on the concentration of diluted transport.

3. RESULTS AND DISCUSSION

The ability and the accuracy of the Hele-Shaw (HS) approximation for modeling fluid flow coupled with the advection-diffusion equation was evaluated by comparing it against results found using the Navier-Stokes equations (NSE). These comparisons were carried out because the NSE is valid for subsurface fluid flow and is, therefore, the gold standard for validating simplified models (Wang et al., 2018). The following results were conducted using a 0.01 Pa pressure difference between the inlet and outlet. Figure 2 compares the averaged concentration calculated by both methods over the surface of the rock fracture, which was extracted from the specified point presented in figure 1. As demonstrated, the evaluated values by the HS method for different rates of surface roughness (the joint roughness coefficient (JRC) in the range of 2.8-7.79) are in good agreement with solved NSE. The prime cause of the small discrepancy is as a consequence of the negligence of inertial forces in the HS approach. The other apparent reason can be attributed to the increased roughness. The generated surface roughness would induce recirculations, which are not accounted for in the HS model. The small decrement of concentration by increasing the JRC has emerged at later times. The possible explanation for this outcome could be that fractures have greater resistance when they are rougher.

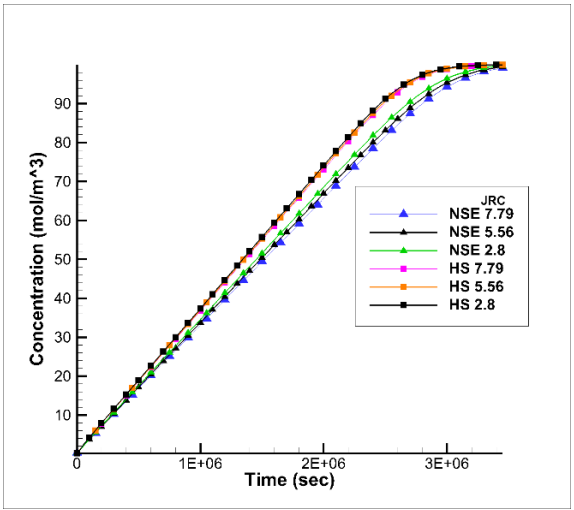

Figure 2: Averaged mineral concentration over fracture surface determined by NSE and HS.

For more clarification, both methods were used for the evaluation of concentration on the generated surface (JRC=0). The determined concentration outlined in Figure 3 was extracted from the red point presented in Figure 1. We observe from Figure 3 that the HS approach has higher accuracy for approximating the concentration in the smooth surface fracture.

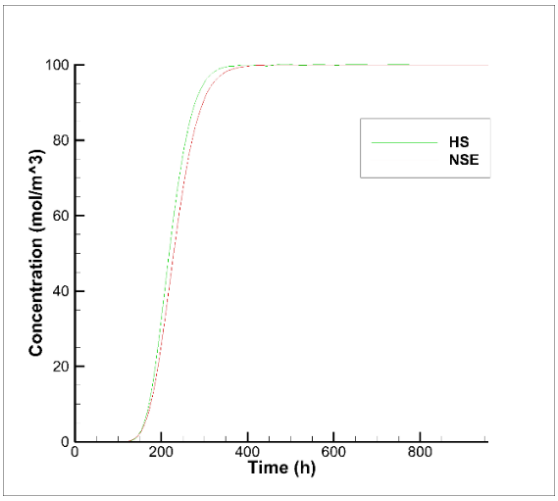

Figure 3: Mineral concentration on the smooth surface fracture evaluated by HS and NSE.

Table 2 summarizes the evaluated average concentration over the surface of the model for HS and the mid-plane for the NSE with different rates of JRC. It is crucial to note that the averaged concentration was calculated at a certain time by both methods, which is 18.5 days. This table is interesting in several ways. First of all, the value of determined concentration by HS approach is slightly greater than the NSE results. Secondly, the error appears to grow slightly as the surface roughness is increased. As reported earlier, the observed decrease of the concentration rate could be interpreted as being a result of greater resistance when the surface is rougher.

Table 2: The effect of different rates of generated surface roughness on mineral concentration.

JRC	HS (mol/m^3)(Concentration)	NSE (mol/m^3) (Concentration)	Error
0.5	59.547	55.376	7%
1.6	59.512	55.287	7%
1.8	59.504	55.257	7%
1.9	59.494	55.236	7%
2.1	59.476	55.185	7%
2.2	59.457	55.129	7%
2.5	59.437	55.073	7%
2.8	59.396	54.969	7%

The concentration contour obtained by the HS approximation is shown in Figure 4. The HS approach is considerably more computationally efficient than the NSE approach; obtaining this result by HS approximation took less than a minute while solving NSE took more than two hours for the same problem.

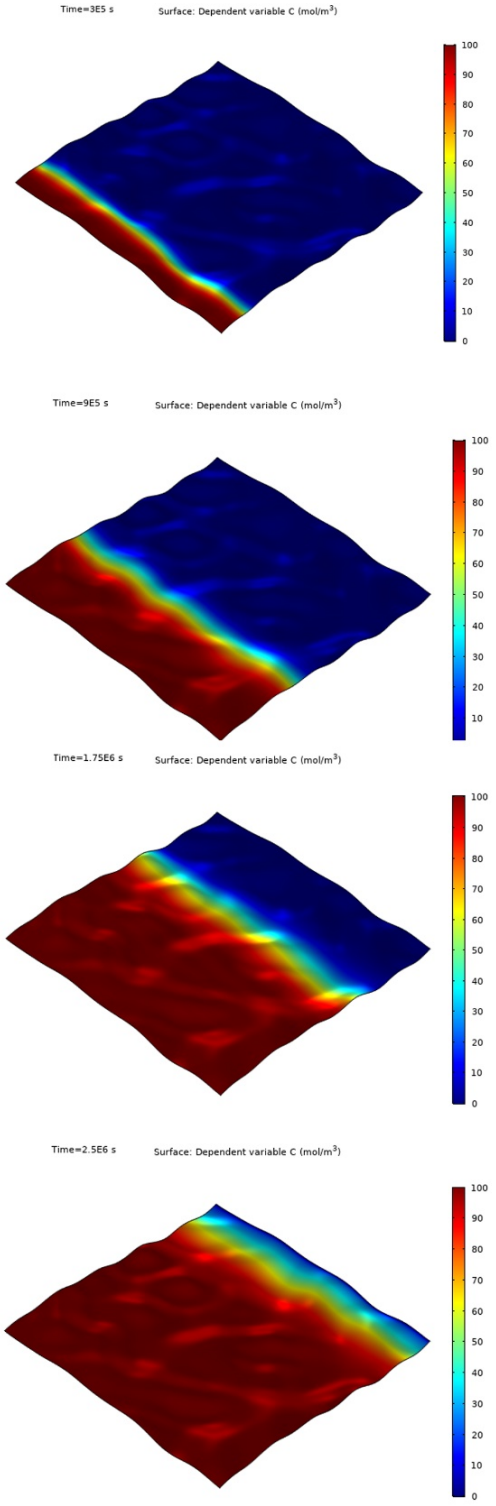

Figure 4: The predicted concentration by HS.

For studying the effect of surface roughness on the flow rate and hydraulic resistance, flow without minerals was simulated. As far as the results show, higher surface roughness cause growth in the hydraulic resistance and reduction in the flow rate, as presented in Table 3. Q_a and Q_b are the calculated flow rates of fluid with NSE and the HS, respectively.

Table 3: The effect of surface roughness on the flow rate and hydraulic resistance.

JRC	Q_a (m^3/s)	Re	$Q_b(m^3/s)$	Err	R $(Pa.s^{-1}.m^{-3})$
0.59	6.35×10^{-6}	6.2	6.6538×10^{-6}	5%	1573.7
3.68	6.33×10^{-6}	6.2	6.6510×10^{-6}	5%	1580.9
4.21	6.30×10^{-6}	6.2	6.6508×10^{-6}	5%	1586.8
5.16	6.23×10^{-6}	6.1	6.65×10^{-6}	6%	1605.3
7.21	6.17×10^{-6}	6.1	6.6494×10^{-6}	7%	1619.8

JRC	$Q_{NSE}(m^3/s)$	**Re**	$Q_{HS}(m^3/s)$	**Err**	R $(Pa.s^{-1}.m^{-3})$
0.59	6.35×10^{-6}	6.2	6.6538×10^{-6}	5%	1573.7
3.68	6.33×10^{-6}	6.2	6.6510×10^{-6}	5%	1580.9
4.21	6.30×10^{-6}	6.2	6.6508×10^{-6}	5%	1586.8
5.16	6.23×10^{-6}	6.1	6.65×10^{-6}	6%	1605.3
7.21	6.17×10^{-6}	6.1	6.6494×10^{-6}	7%	1619.8

4. CONCLUSION

In this research, a computationally efficient approach was developed for studying the effect of fracture-surface roughness on solute transport. To prove the validity of the Hele-Shaw (HS) approximation, Navier-Stokes equations (NSE) were used as a benchmark. For modeling solute transport, we applied the advection-diffusion equation coupled with the flow-fields provided by the HS and NSE approaches. The evaluated results from the HS method are in good agreement with the NSE (7% Error). It is worthwhile noting that results have been obtained by HS in less than 1 minute while solving NSE took more than two hours for the same physical geometry. This remarkable reduction in computational time is the most important achievement of this research and it enables us to simulate solute transport in realistically large fracture networks. As anticipated, the average concentration decreases by increasing the surface roughness. Interestingly, the hydraulic resistance rises with the higher surface roughness. We believe that our method could be usefully employed in studying the effect of diluted species transport in a network of rock fractures. This finding is one of the prime steps for studying silica scaling in fracture networks, which can be achieved by patching HS cells.

REFERENCES

Barnsley, M.F., Devaney, R.L., Mandelbrot, B.B., Peitgen, H.O., Saupe, D., Voss, R.F., Fisher, Y.. McGuire, M.: *The Science of Fractal Images*. Springer. (1988).

Bundschuh, J., Suárez Arriaga, M.C: *Introduction to the Numerical Modeling of Groundwater and Geothermal Systems: Fundamentals of Mass, Energy and Solute Transport in Poroelastic Rocks*. CRC Press. (2010).

de Castro, C.P., Luković, M., Andrade, R.F.S., Herrmann, H. J.: The influence of statistical properties of Fourier coefficients on random Gaussian surfaces. *Scientific Reports*, *7*. (2017).

Fabbro, V., Bourlier, C., Combes, P.F.: Forward propagation modeling above Gaussian rough surfaces by the parabolic wave equation: Introduction of the shadowing effect. *Progress In Electromagnetics Research*, *58*, 243–269. (2006).

Feng, G., Kang, Y., Meng, T., Hu, Y.Q., Li, X.H.: The influence of temperature on mode I fracture toughness and fracture characteristics of sandstone. *Rock Mechanics and Rock Engineering*, *50*(8), 2007–2019. (2017).

Gepner, S.W., Floryan, J.M.: Use of Surface Corrugations for Energy-Efficient Chaotic Stirring in Low Reynolds Number Flows. *Scientific reports*, *10*. (2020).

Huang, B., Cova, T.J., Tsou, M.H., Bareth, G., Song, C., Song, Y., Cao, K., Silva, E.A.: *Comprehensive Geographic Information Systems*. Elsevier. (2017).

Li, B., Liu, R., Jiang, Y.: Influences of hydraulic gradient, surface roughness, intersecting angle, and scale effect on nonlinear flow behavior at single fracture intersections. *Journal of Hydrology*, *538*, 440–453. (2016).

Patir, N.: A numerical procedure for random generation of rough surfaces. *Wear*, *47*(2), 263–277. (1978).

Peitgen, H.O., Jürgens, H., Saupe, D.: *Chaos and Fractals: New Frontiers of Science*. Springer. (2004).

Wang, Z., Xu, C., Dowd, P.: A modified cubic law for single-phase saturated laminar flow in rough rock fractures. *International Journal of Rock Mechanics and Mining Sciences*, *103*, 107–115. (2018).

Wu, Z., Fan, L., Zhao, S.: Effects of hydraulic gradient, intersecting angle, aperture, and fracture length on the nonlinearity of fluid flow in smooth intersecting fractures: An experimental investigation. *Geofluids*, *2018*. (2018).

Yu, L., Liu, R., Jiang, Y.: A review of critical conditions for the onset of nonlinear fluid flow in rock fractures. *Geofluids*, *2017*. (2017).

Zhang, G., Karakus, M., Tang, H., Ge, Y., Jiang, Q.: Estimation of joint roughness coefficient from three-dimensional discontinuity surface. *Rock Mechanics and Rock Engineering*, *50*(9), 2535–2546. (2017).

Zhou, Z., Su, Y., Wang, W., Yan, Y.: Application of the fractal geometry theory on fracture network simulation. *Journal of Petroleum Exploration and Production Technology*, *7*(2), 487–496. (2017).

ISSN 2703-4275